On the use of manometry method for measurement of gas adsorption equilibria and characterization of clay texture with Derivative Isotherm Summation

Denys Grekov, Pascaline Pre, Bernd Grambow

HAL Id: in2p3-02413260
https://hal.in2p3.fr/in2p3-02413260

Submitted on 21 Jul 2022

1   On the use of manometry method for measurement of gas adsorption equilibria and

2   characterization of clay texture with Derivative Isotherm Summation.

3

4   Denys Grekov,[a*] Pascaline Pré,[b] Bernd Grambow[a]

5   [a] SUBATECH (IMT Atlantique, Université de Nantes, CNRS-IN2P3), F-44307 Nantes,

6   France

7   [b] IMT Atlantique, GEPEA UMR CNRS 6144, F-44307 Nantes, France

8   Corresponding author: denys.grekov@imt-atlantique.fr

9   **Abstract**

10   Gas adsorption is widely used for characterization of clays. Apart from "classical" experiment

11   of nitrogen or other gases adsorption/desorption at cryogenic temperatures, allowing the

12   determination of the specific surface area, partial mesopore and micropore volume and size

13   distributions, gas adsorption can also be used for the characterization of clay surface texture

14   (energetic heterogeneity) related to layered structure of clays. Derivative Isotherm Summation

15   applied to high-resolution gas adsorption isotherms was shown to be a powerful tool to access

16   energetic characteristics and ratio between basal and lateral faces of clay particles. To date,

17   the method is not commonly employed for characterization of clays and other heterogeneous

18   solids, probably due to specificity of high-resolution isotherms acquisition technique

19   described in the original literature: quasi-equilibrium volumetry with gas injection by

20   microleak. We illustrated in the present work a possibility to use widely available static

21   manometric commercial gas adsorption analysers for this purpose.

22   **Keywords:** clay particles; basal faces; lateral faces; gas adsorption; derivative isotherm

23   summation.

1. Introduction

Clay particles feature a specific texture originating from the coexistence of structurally inequivalent basal (pyrophilite-like) and lateral (hydroxylated) faces. These influence properties of clays such as cation exchange capacity, chemical species retention, zeta potential etc. (Bradbury and Baeyens, 2000; Hassan et al., 2005; Leroy et al., 2015). Atomic force microscopy (AFM) and electron microscopy image reconstruction (Ploehn et al., 2000; Tournassat et al., 2003; Cadene et al., 2005; Sayed Hassan et al., 2006) and Derivative Isotherm Summation (DIS) (Bardot et al., 1998; Michot and Villiéras, 2002) have emerged as accurate tools to characterize the texture of clay surfaces. While the former technique is well-known and currently utilized for characterization of clays and other layered solids, the application of the latter one is less common. A detailed description of DIS method can be found in the original literature and reviews (Villiéras et al., 1992, 1997, 2002; Nir et al., 2006). Here we only briefly recall the basic principle of DIS in the context of clays surface characterization.

Michot et al. illustrated that for majority of clays, upon Ar or N_2 adsorption at 77 K, the monolayer completion occurs first on highly polarizing lateral faces (at lower pressures) and then on basal surfaces (at higher pressures) (Michot et al., 1990). Quasi-equilibrium volumetry (or more precisely manometry) with gas injection by micro-leak was proposed for the acquisition of high-resolution isotherms composed of more than 2000 experimental points in the domain of relative pressures ranging between 10^{-7} and 0.1. This technique offers the advantage of detecting progressive monolayer completion on different surface domains and usually allows the acquisition of very smooth isotherms. Villieras et al. have further proposed to simulate the derivatives of high-resolution isotherms, being more sensitive to fine variations of adsorbed amount, especially in the case of multi-component isotherms, with the sum of theoretical monolayer or multilayer adsorption isotherm derivatives in order to access

49   energetic parameters of adsorption and areas of individual surface domains (DIS procedure)

50   (Villiéras et al., 1992). A very similar procedure for the calculation of adsorption potential

51   distribution was introduced earlier by Jaroniec and Choma (Jaroniec and Choma, 1987) for

52   the characterization of microporous materials (Jaroniec et al., 1996; Jaroniec and Choma,

53   1997). The most commonly employed models for isotherm simulation in the context of DIS

54   for the characterization of clays are Bragg-Williams-Temkin (BWT) (1) and Brunauer-

55   Emmett-Teller-Hill (BET-H) (2) equations describing monolayer and multilayer adsorption

56   respectively. According to these models, the coverage of adsorption sites θ (related to

57   adsorbed amount V_{ads}) with relative gas pressure ($p/p°$) is influenced by adsorbate/adsorbent

58   and lateral adsorbate/adsorbate interactions, which are described respectively with the

59   parameters C and ω. More details are given in (Villiéras et al., 1997). Equation (1) is usually

60   retained for the description of low-pressure components. Its derivative in $\ln(p/p°)$ –

61   $dV_{ads}/d\ln(p/p°)$ coordinates affords symmetric peaks with the position and width being

62   determined by C and ω respectively. The derivative of equation (2) leads to peaks with

63   ascending right-hand side and is mostly used for the description of high-pressure components

64   where multilayer adsorption takes place. Other models for the description of adsorption on

65   planar surfaces and in micropores (Dubinin-Astakhov equation and its extensions) are also

66   available (Villiéras et al., 1997). Due to its quadrupolar momentum, nitrogen specifically

67   interacts with cations or other chemical species such as surface hydroxyl groups and may be

68   differently oriented near these sites, making isotherm analysis difficult. Thus, monoatomic

69   gases like argon, characterized by spherical geometry are preferred probes for surface texture

70   analysis.

71
$$\theta = \frac{C \cdot \exp\left(\frac{\omega \cdot \theta}{kT}\right) \cdot exp(ln(p/p°))}{1 + C \cdot \exp\left(\frac{\omega \cdot \theta}{kT}\right) \cdot exp(ln(p/p°))} \quad (1)$$

$$72 \qquad \theta = \frac{C \cdot \exp\left(\frac{\omega \cdot \theta}{kT}\right) \cdot exp\left(ln(p/p°)\right)}{\left[1 - exp\left(ln(p/p°)\right)\right] \cdot \left[1 + \left(C \cdot \exp\left(\frac{\omega \cdot \theta}{kT}\right) - 1\right) \cdot exp\left(ln(p/p°)\right)\right]} \qquad (2)$$

73 DIS was illustrated to be a powerful tool for surface heterogeneity analysis, and it was

74 extensively applied by Villieras and co-authors for the characterization of different families of

75 clays and other minerals and synthetic materials, such as nanocrystalline or microporous

76 solids (Bardot et al., 1998; Michot and Villiéras, 2002; Prélot et al., 2003b, 2003a; Garnier et

77 al., 2007; Ali Ahmad et al., 2013). Nowadays, the DIS technique is not commonly employed,

78 probably due to the specificity of the equipment proposed in the original literature for the

79 acquisition of high-resolution isotherms smooth enough to obtain interpretable derivatives. In

80 the present contribution, we evaluate the applicability of the DIS procedure to high-resolution

81 isotherms obtained with available commercial gas adsorption analysers in the context of clay

82 surfaces heterogeneity analysis, using Argon adsorption at 77 K.

83 **2. Materials and methods**

84 **Gas adsorption isotherm measurement.** The isotherms were acquired using 3Flex

85 automated static manometric adsorption analyser from Micromeritics, equipped with high

86 accuracy pressure transducers (precision 0.15 % of absolute pressure reading) allowing for

87 measurements in the domain of Argon or Nitrogen relative pressure ranging between 10^{-6}-10^{-7}

88 and 1. Such a broad range of pressures is required for characterization of micro- and

89 mesopores. The acquisition was performed in fixed-dose mode, varying the amount of

90 injected gas between 0.01 and 10 cm^3/g, depending on pressure interval and specific surface

91 area of analysed samples. In the same way, the equilibration time after gas injection was

92 adjusted and optimized by varying the pressure measurement interval from 10 up to 90 s. The

93 optimization procedure consists of the research of experimental conditions where the

94 thermodynamic equilibrium of adsorption is attained and completely smooth isotherm,

95   featuring at least 10-20 points per decade of gas pressure values, is acquired within 48-60 h,

96   which corresponds to the autonomy time of the Dewar vessel filled with liquid nitrogen to

97   maintain cryogenic temperature in the sample tube. As an example, for Illite du Puy featuring

98   specific surface area close to 100 m^2/g we found the following amounts of injected Ar

99   allowing the generation of sufficiently high number of experimental points per domain of

100   values of gas pressures: 0.015 cm^3/g until p/p°=$2\cdot10^{-5}$, then 0.05 cm^3/g until p/p°=$2\cdot10^{-4}$, then

101   0.15 cm^3/g until p/p°=10^{-3}, then 0.2 cm^3/g until p/p°=10^{-2}, 0.6 cm^3/g until p/p°=10^{-1} and

102   finally 5 cm^3/g until p/p°=$3\cdot10^{-1}$. Pressure measurement interval during equilibration

103   processes was set to 15 s for relative pressures ranging between $2\cdot10^{-5}$ and $3\cdot10^{-1}$, its

104   prolongation did not significantly influence the isotherm shape. Since at low pressure the

105   equilibration kinetics is slow this parameter was fixed to 30 s below p/p°=$2\cdot10^{-5}$ in order to

106   avoid s-shaped artefact. The saturated vapour pressure of Argon at 77 K was measured

107   periodically. Specific surface areas were determined from Ar adsorption isotherms using BET

108   theory (adsorbed Ar cross section area at 77 K – 0.143 nm^2) in the domain of relative

109   pressures 0.1-0.3. Before isotherms measurements, all samples were outgassed under dynamic

110   vacuum at 393 K until residual pressure stabilization (at least 72 h). The volumes of cells non-

111   occupied by samples were determined at ambient temperature and at 77 K by He expansion.

112   The derivatives of experimentally measured isotherms were calculated using numerical

113   procedure. Only smooth isotherms afford "high-quality" interpretable derivatives. Those were

114   simulated with the sum of derivatives determined from the equations (1) and (2). For low-

115   pressure domains, we mainly considered BWT equation (monolayer adsorption) while for

116   high-pressure domain, where multilayer adsorption takes place – BET-H equation. Both

117   equations were resolved using an iterative method for each experimentally measured point of

118   pressure whilst their derivatives were computed by differentiation. The number of

119   components needed to simulate experimental isotherm derivatives, their weight and

120   parameters C and ω were adjusted as best-fit parameters minimising the residual sum of

121   squares between experimental and simulated isotherms, as recommended in (Villiéras et al.,

122   1997). The weight of the individual components corresponds to their contribution to the total

123   specific surface area of the solid. In the specific case of clays, the contribution (fraction) of

124   surfaces of basal faces to the total specific surface area (composed of basal and lateral faces)

125   corresponds to the lamillarity index (L) which quantitatively describes their texture.

126   **Sample preparation.** A fine (< 2 µm) montmorillonite fraction was extracted from Bentonite

127   MX-80 by 5 g/l suspension centrifugation at 1000 rpm and it was further exchanged with Na

128   by following the standard procedure: contact with 0.5 mol/l NaCl solution, 6 cycles of

129   centrifugation at 20000 rpm and subsequent washing/re-dispersion in deionized water and

130   suspension drying at 323 K under air. The clay fraction from Illite du Puy was purified by an

131   elutriation procedure and further transformed to a Na-exchanged form in the same way as a

132   montmorillonite sample (Tournassat et al., 2007). Kaolinite was received from Fluka

133   Analytical (Sigma Aldrich) in form of fine powder (<150 μm) and analysed without any

134   purification. Two core samples of natural clay-rock come from the Callovo-Oxfordian

135   mudstones, East of Paris basin, underground laboratory of Bure, France (Gaucher et al.,

136   2004). Both samples are characterized by the same clay fraction content (about 45%)

137   featuring different composition (COx-EST 48599 (-508,3 m): 75-80% of illite and 20-25% of

138   smectite, COx-EST 48601 (-466 m): 60-70% of illite and 30-40% of smectite). All samples

139   except kaolinite (already powdered) were grinded manually and sieved to collect < 100 µm

140   size fraction.

141   **3. Results and discussion**

142   In a first step high-resolution Ar adsorption isotherms were acquired for three pure-phase

143   "model" clays: kaolinite, illite and montmorillonite, extensively studied by the DIS technique

144   (Villiéras et al., 1997; Bardot et al., 1998; Tournassat et al., 2003; Sayed Hassan et al., 2006).

145 The experimental isotherms and their derivatives are shown in Figure 1. All isotherm

146 derivatives feature a classical shape as observed earlier, including a major component

147 characterized by a peak at $\ln(p/p°)\approx$ -4..-5 and a more or less pronounced secondary

148 component in the range of lower pressures, merging as a shoulder at $\ln(p/p°)\approx$ -8..-6, as well

149 as a minor component below -10. Isotherm deconvolution with BWT and BET-H models

150 reveals an overlap of these different contributions. According to the bibliographic results

151 (Sayed Hassan et al., 2006), low-energy (high-pressure) and high-energy (low-pressure)

152 components are assigned, with some exceptions (Villiéras et al., 1997, 2002), to basal (b) and

153 lateral (l) faces respectively. The lamellarity index (L) determined by the degree of layers

154 stacking is used for quantitative description of clays texture. For kaolinite and illite the shapes

155 of isotherms and deduced energetic parameters of argon adsorption on different surface

156 domains (C and ω) are close to those reported in the literature (Table 1) (Sayed Hassan et al.,

157 2006). For montmorillonite extracted from bentonite MX-80, however, the isotherm envelop

158 slightly differs: low-pressure components, related to the contribution of lateral faces, feature a

159 more pronounced character when compared to that described by Tournassat et al. (Tournassat

160 et al., 2003). A similar signature was observed for Na-SWy-1 montmorillonite (Le Forestier et

161 al., 2010). The difference in textural properties of montmorillonites can be related to sample

162 preparation procedure. In the present work clay suspension was air dried while in (Tournassat

163 et al., 2003) it was freeze-dried and according to (Pacuła et al., 2006), freeze-drying may

164 influence surface areas and texture of swelling clays.

165 We further probed the use of equilibrium manometry for high-resolution Ar adsorption

166 isotherms acquisition for natural clay rock samples texture analysis. Isotherm derivatives

167 together with their best-fit simulation (BWT and BET-H models) for COx-EST 48599 and

168 COx-EST 48601 argillite are represented in Figure 2. The shapes of the isotherms are similar

169 to those of pure-phase clays. In spite of the closeness of structural features of single-phase

170 clays and argillite clay fraction (Tournassat et al., 2009), the components of the isotherms

171 accessed by best-fit simulation are assigned to the same surface sites as in cases of reference

172 systems, i.e. low-pressure components – lateral faces, high-pressure components – basal

173 faces. While low-pressure components of both isotherms feature almost identical intensity, the

174 high-pressure main component in case of COx-EST 48601 isotherm is less pronounced in

175 comparison to COx-EST 48599. This suggests a lower contribution of basal faces to the total

176 specific surface area for former argillite. Energetic parameters determined by isotherm

177 simulation are summarized in Table 1.

178 Comparing the lamellarity indexes for pure-phase clays, one can realize that in case of

179 montmorillonite sample, characterized by low value of L and consequently low contribution

180 of basal faces to the total specific surface area (Table 1), the stacking of phyllosilicate sheets

181 is higher than for illite or kaolinite featuring higher L values. Interestingly, the same trend is

182 also observed for natural clay rock samples. For instance, COx-EST 48601, which features

183 higher smectite fraction content, is characterized by lower lamellarity index and thus higher

184 level of phyllosilicate sheets stacking acquired during diagenesis in comparison to COx-EST

185 48599.

186   **4. Conclusion**

187 High-resolution Ar adsorption isotherms were acquired at 77 K for a series of model single-

188 phase clays and complex natural argillite samples using static manometry method. High-

189 quality derivatives were obtained for the entire set of samples despite significantly lower

190 number of measured experimental points (on the order of 150-250) in comparison to isotherm

191 acquisition by quasi-equilibrium manometry with gas injection by micro-leak (more than

192 2000 points). Simulation of measured isotherms derivatives with the sum of derivatives of

193 theoretical isotherms computed with the BWT and BET-H models afforded energetic

194 parameters and areas of basal and lateral faces of clay particles. The shapes of measured

195   isotherms, energetic parameters and textural properties accessed for model single-phase clays

196   were found to be in a good agreement with those for similar systems described in the

197   literature. This illustrates a possibility of using commercial gas adsorption analysers for clays

198   surfaces texture characterization by DIS technique, making indeed the method more

199   accessible. By analysing natural clay rock samples with this approach, we confirmed the

200   relationship between illite/smectite ratio and the degree of phyllosilicate layer staking,

201   quantitatively described by lamellarity index. One should notice that a possibility of natural

202   argillite texture characterization without specific sample preparation is a great advantage of

203   DIS in comparison to AFM image reconstruction technique.

References

208   Ali Ahmad, M., Prelot, B., Dufour, F., Durupthy, O., Razafitianamaharavo, A., Douillard,

209   J.M., Chaneac, C., Villiéras, F., Zajac, J., 2013. Influence of morphology and

210   crystallinity on surface reactivity of nanosized anatase TiO2 studied by adsorption

211   techniques. 2. solid-liquid interface. J. Phys. Chem. C 117, 4459–4469.

212   https://doi.org/10.1021/jp3077084

213   Bardot, F., Villiéras, F., Michot, L.J., François, M., Gérard, G., Cases, J.M., 1998. High

214   resolution gas adsorption study on illites permuted with various cations: Assessment of

215   surface energetic properties. J. Dispers. Sci. Technol. 19, 739–759.

216   https://doi.org/10.1080/01932699808913212

217   Bradbury, M.H., Baeyens, B., 2000. A generalised sorption model for the concentration

218   dependent uptake of caesium by argillaceous rocks. J. Contam. Hydrol. 42, 141–163.

219   https://doi.org/10.1016/S0169-7722(99)00094-7

220   Cadene, A., Durand-Vidal, S., Turq, P., Brendle, J., 2005. Study of individual Na-

221   montmorillonite particles size, morphology, and apparent charge. J. Colloid Interface

222   Sci. 285, 719–730. https://doi.org/10.1016/j.jcis.2004.12.016

223   Garnier, C., Görner, T., Villiéras, F., De Donato, P., Polakovič, M., Bersillon, J.L., Michot,

224   L.J., 2007. Activated carbon surface heterogeneity seen by parallel probing by inverse

225   liquid chromatography at the solid/liquid interface and by gas adsorption analysis at the

226   solid/gas interface. Carbon N. Y. 45, 240–247.

227   https://doi.org/10.1016/j.carbon.2006.10.004

228   Gaucher, E., Robelin, C., Matray, J.M., Négrel, G., Gros, Y., Heitz, J.F., Vinsot, A., Rebours,

229   H., Cassagnabère, A., Bouchet, A., 2004. ANDRA underground research laboratory:

230   Interpretation of the mineralogical and geochemical data acquired in the Callovian-

231   Oxfordian formation by investigative drilling. Phys. Chem. Earth 29, 55–77.

232   https://doi.org/10.1016/j.pce.2003.11.006

233   Hassan, M.S., Villiéras, F., Razafitianamaharavo, A., Michot, L.J., 2005. Role of

234   exchangeable cations on geometrical and energetic surface heterogeneity of kaolinites.

235   Langmuir 21, 12283–12289. https://doi.org/10.1021/la051993n

236   Jaroniec, M., Choma, J., 1997. Characterization of geometrical and energetic heterogeneities

237   of active carbons by using sorption measurements. Equilibria Dyn. Gas Adsorpt.

238   Heterog. Solid Surfaces Stud. Surf. Sci. Catal. 104, 715–744.

239   Jaroniec, M., Choma, J., 1987. Characterization of activated carbons by distribution functions

240   of adsorption potential and micropore dimension. Mater. Chem. Phys. 18, 103–117.

241   https://doi.org/10.1016/0254-0584(87)90115-5

242   Jaroniec, M., Gadkaree, K.P., Choma, J., 1996. Relation between adsorption potential

243   distribution and pore volume distribution for microporous carbons. Colloids Surfaces A

244   Physicochem. Eng. Asp. 118, 203–210. https://doi.org/10.1016/S0927-7757(96)03685-0

245   Le Forestier, L., Muller, F., Villieras, F., Pelletier, M., 2010. Textural and hydration

246   properties of a synthetic montmorillonite compared with a natural Na-exchanged clay

247   analogue. Appl. Clay Sci. 48, 18–25. https://doi.org/10.1016/j.clay.2009.11.038

248   Leroy, P., Tournassat, C., Bernard, O., Devau, N., Azaroual, M., 2015. The electrophoretic

249   mobility of montmorillonite. Zeta potential and surface conductivity effects. J. Colloid

250   Interface Sci. 451, 21–39. https://doi.org/10.1016/j.jcis.2015.03.047

251   Michot, L., Francois, M., Cases, J.M., 1990. Surface Heterogeneity Studied by a Quasi-

252   Equilibrium Gas Adsorption Procedure. Langmuir 6, 677–681.

253   https://doi.org/10.1021/la00093a025

254   Michot, L.J., Villiéras, F., 2002. Assessment of surface energetic heterogeneity of synthetic

255   Na- saponites. The role of layer charge. Clay Miner. 37, 39–57.

256   https://doi.org/10.1180/0009855023710016

257   Nir, S., El Nahhal, Y., Undabeytia, T., Rytwo, G., Polubesova, T., Mishael, Y., Rabinovitz,

258   U., Rubin, B., 2006. Handbook of Clay Science, Developments in Clay Science.

259   https://doi.org/10.1016/S1572-4352(05)01021-4

260   Pacuła, A., Bielańska, E., Gaweł, A., Bahranowski, K., Serwicka, E.M., 2006. Textural effects

261   in powdered montmorillonite induced by freeze-drying and ultrasound pretreatment.

262   Appl. Clay Sci. 32, 64–72. https://doi.org/10.1016/j.clay.2005.10.002

263   Ploehn, H.J., Liu, C., Scrivens, W.A., Loye, H., 2000. Quantitative Analysis of Platelet Size

264   by Atomic Force Microscopy 1–4.

265   Prélot, B., Villiéras, F., Pelletier, M., Gérard, G., Gaboriaud, F., Ehrhardt, J.J., Perrone, J.,

266   Fedoroff, M., Jeanjean, J., Lefèvre, G., Mazerolles, L., Pastol, J.L., Rouchaud, J.C.,

267   Lindecker, C., 2003a. Morphology and surface heterogeneities in synthetic goethites. J.

268   Colloid Interface Sci. 261, 244–254. https://doi.org/10.1016/S0021-9797(03)00058-4

269   Prélot, B., Villiéras, F., Pelletier, M., Razafitianamaharavo, A., Thomas, F., Poinsignon, C.,

270   2003b. Structural–chemical disorder of manganese dioxides. J. Colloid Interface Sci.

271   264, 343–353. https://doi.org/10.1016/s0021-9797(03)00394-1

272   Sayed Hassan, M., Villieras, F., Gaboriaud, F., Razafitianamaharavo, A., 2006. AFM and

273   low-pressure argon adsorption analysis of geometrical properties of phyllosilicates. J.

274   Colloid Interface Sci. 296, 614–623. https://doi.org/10.1016/j.jcis.2005.09.028

275   Tournassat, C., Gailhanou, H., Crouzet, C., Braibant, G., Gautier, A., Gaucher, E.C., 2009.

276   Cation Exchange Selectivity Coefficient Values on Smectite and Mixed-Layer

277   Illite/Smectite Minerals. Soil Sci. Soc. Am. J. 73, 928.

278   https://doi.org/10.2136/sssaj2008.0285

279   Tournassat, C., Gailhanou, H., Crouzet, C., Braibant, G., Gautier, A., Lassin, A., Blanc, P.,

280   Gaucher, E.C., 2007. Two cation exchange models for direct and inverse modelling of

281   solution major cation composition in equilibrium with illite surfaces. Geochim.

282   Cosmochim. Acta 71, 1098–1114. https://doi.org/10.1016/j.gca.2006.11.018

283   Tournassat, C., Neaman, A., Villéras, F., Bosbach, D., Charlet, L., 2003. Nanomorphology of

284   montmorillonite particles: Estimation of the clay edge sorption site density by low-

285   pressure gas adsorption and AFM observations. Am. Mineral. 88, 1989–1995.

286   Villiéras, F., Cases, J.M., François, M., Michot, L.J., Thomas, F., 1992. Texture and Surface

287   Energetic Heterogeneity of Solids from Modeling of Low Pressure Gas Adsorption

288   Isotherms. Langmuir 8, 1789–1795. https://doi.org/10.1021/la00043a018

289   Villiéras, F., Michot, L.J., Bardot, F., Cases, J.M., François, M., Rudziński, W., 1997. An

290   Improved Derivative Isotherm Summation Method To Study Surface Heterogeneity of

291   Clay Minerals †. Langmuir 13, 1104–1117. https://doi.org/10.1021/la9510083

292 Villiéras, F., Michot, L.J., Bardot, F., Chamerois, M., Eypert-Blaison, C., François, M.,

293   Gérard, G., Cases, J.-M., 2002. Surface heterogeneity of minerals. Comptes Rendus

294   Geosci. 334, 597–609. https://doi.org/10.1016/s1631-0713(02)01799-6

295
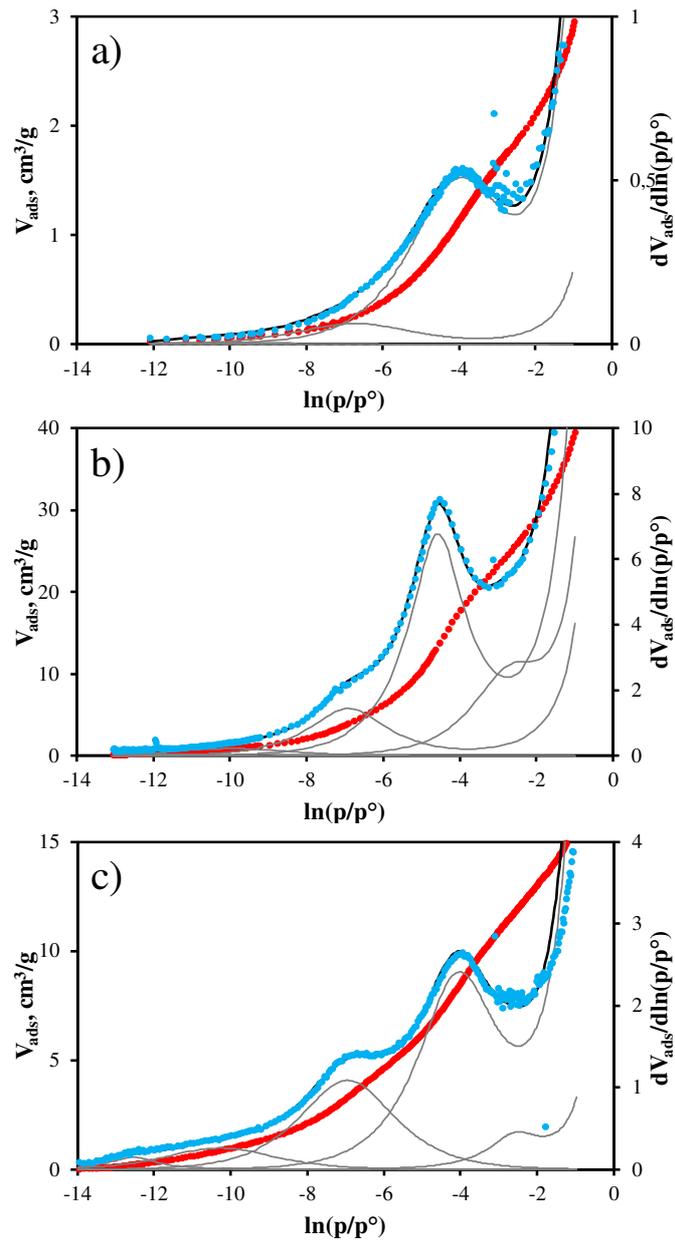
Figure 1. Isotherms (red points) of argon adsorption at 77 K and corresponding derivatives (blue points) together with their best-fit simulations (black line) and individual contributions (grey lines) for: a) kaolinite, b) illite and c) montmorillonite.
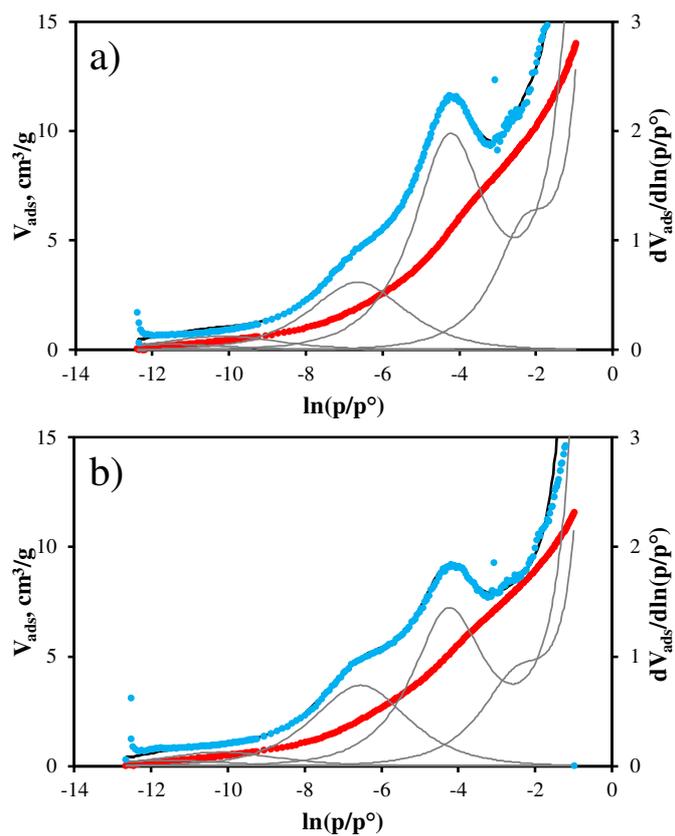
Figure 2. Isotherms (red points) of argon adsorption at 77 K and corresponding derivatives (blue points) together with their best-fit simulations (black line) and individual contributions (grey lines) for: a) COx-EST 48599 and b) COx-EST 48601 clay rock samples.

Table 1. Energetic parameters and areas of different domains of clays surfaces determined by DIS procedure applied to high-resolution Ar adsorption isotherms.

Component	I (b)	II (b)	III (l)	IV (l)	V (l)
Kaolinite (Fluka) S_{BET}=7.6 m²/g, L=0.85					
Position		-3.7	-6.9	-9.7	
S_i, m²/g		6.4	1	0.2	
C		44	800	20·10³	
ω		0.5	0	0	
*Kaolinite (Kga2) (Sayed Hassan et al., 2006) S_{BET}=21 m²/g, L=0.84					
Position	-2.2	-3.8	-6.8	-9.7	
S_i, m²/g	3.8	13.9	2.3	0.5	
ω	0	1.3	-0.8	0	
Illite du Puy-Na S_{BET}=108 m²/g, L=0.8					
Position	-2.4	-4.4	-6.9	-10.1	-12
S_i, m²/g	25	61	16.5	3.6	1.4
C	9	42	550	20·10³	50·10⁴
ω	1	1.6	1.1	0	0
*Illite du Puy-Na (Sayed Hassan et al., 2006) S_{BET}=171 m²/g, L=0.78					
Position	-2.6	-4.5	-6.9	-10.1	-13
S_i, m²/g	61.4	71.2	29.7	7.5	0.7
ω	0	1.7	0.5	0	0.5
Montmorillonite-Na S_{BET}=45 m²/g, L=0.6					
Position	-2.3	-3.9	-6.8	-10.4	-12.6
S_i, m²/g	2.9	24.1	13.3	3.6	1.1
C	6	35	750	25·10³	10·10⁴
ω	1.5	1	0.6	0.2	1
*Montmorillonite SWy-2-Na (Le Forestier et al., 2010) S_{BET}=47 m²/g, L=0.47					
Position	-2.7	-4.4	-7	-9.6	
S_i, m²/g	2.6	19.2	20.6	4.8	
*Bentonite MX-80 (Tournassat et al., 2003) S_{BET}=35 m²/g, L=0.75					
Position	-2.5	-4.1	-7	-10.3	
S_i, m²/g	2	24.6	5.6	2.9	
COx-EST 48599 S_{BET}=37 m²/g, L=0.72					
ln(p/p°)	-2.1	-4.1	-6.6	-10.2	-11.5
S_i, m²/g	8	18.8	7.6	1.8	0.8
C	5.5	38	550	25·10³	10·10⁴
ω	1.2	1.2	0.6	0	0
COx-EST 48601 S_{BET}=31 m²/g, L=0.65					
Position	-2.3	-4.1	-6.5	-10.2	-11.5
S_i, m²/g	6.6	13.2	8.7	1.7	0.7
C	7.5	38	500	25·10³	10·10⁴
ω	1	1.2	0.6	0	0

b – basal faces, l – lateral faces, * – bibliographic data.